

**Energy Impact of Ventilation and Air Infiltration
14th AIVC Conference, Copenhagen, Denmark
21-23 September 1993**

Flow of Aerosol Particles Through Large Openings

N M Adam, S B Riffat

**Building Technology Group, School of Architecture
University of Nottingham, University Park Nottingham,
NG7 2RD, UK**

FLOW OF AEROSOL PARTICLES THROUGH LARGE OPENINGS

SYNOPSIS

The first part of this paper describes a detailed study of the flow of aerosol particles through large openings and the second part describes deposition characteristics of aerosol particles in a single-zone chamber lined with different types of materials, e.g. aluminium foil and carpet.

Tracer-gas and aerosol particles were injected into a naturally ventilated room and their concentrations with time were monitored. The room was fitted with a number of windows which allowed examination of single-sided ventilation. The behaviour of particles within the zone with respect to mixing, age-of-particles and particle effectiveness was also examined. The deposition rate of particles was found to be dependent on the type of lining material and size of particles used. Results indicated that particle exchange rates were higher than tracer-gas exchange rates.

LIST OF SYMBOLS

- $C_{g(t)}$ = concentration tracer-gas ($\mu\text{g}/\text{m}^3$ or ppm) at time t
 $C_{g(0)}$ = concentration tracer-gas ($\mu\text{g}/\text{m}^3$ or ppm) at time t equals zero
 $C_{p(t)}$ = concentration aerosol particle ($\mu\text{g}/\text{m}^3$ or ppm) at time t
 $C_{p(0)}$ = concentration aerosol particle ($\mu\text{g}/\text{m}^3$ or ppm) at time t equals zero
 d = particle diameter (μm)
 I = tracer-gas exchange rate ($\mu\text{g}/\text{m}^3\text{h}$ or h^{-1})
 P = particle-exchange rate ($\mu\text{g}/\text{m}^3\text{h}$ or h^{-1})
 C_0 = concentration measurement at time t equals zero ($\mu\text{g}/\text{m}^3$ or ppm)
 C_j = concentration measurement at j ($\mu\text{g}/\text{m}^3$ or ppm)
 C_M = final concentration measured ($\mu\text{g}/\text{m}^3$ or ppm)
 M = number of measurements
 $\Delta\tau$ = sampling interval (min)
 λ_{exp} = slope in the exponential decay region
 τ_j = time of measurement j (min)
 τ_M = total measuring time, $\tau_M = M \cdot \Delta\tau$ (min)
 α = particle deposition rate ($\mu\text{g}/\text{m}^2\text{h}$)
 V = volume of room (m^3)
 A = total surface area of room (m^2)
 H = height of sampling point from floor (m) [See Figure 1]
 X = location of sampling point from side window (m) [See Figure 1]

| | |
|--------------|---|
| τ_{LT} | =local age-of-tracer (min) |
| τ_{AT} | =average age-of-tracer (min) |
| τ_{LP} | =local age-of-particle (min) |
| τ_{AP} | =average age-of-particle (min) |
| ϵ_i | =local tracer or particle-exchange indicator (%) |
| τ_n | =the system's average nominal time constant (min) |
| τ_p | =the local age-of-tracer (or particles) at a point (min) |
| w_s | =wind speed (m/s) |
| w_D | =wind direction (degrees N) |
| ΔT | =indoor temperature - outdoor temperature ($^{\circ}C$) |
| V_D | =deposition velocity (cm/s) |

1. INTRODUCTION

Particulate pollutants in buildings can have damaging effects on the health of the occupants and studies have shown that indoor aerosol particles strongly influence the incidence of sick building syndrome [1]. Indoor aerosols are not only associated with outdoor sources (e.g. car exhaust emissions, coal and oil combustion, road dust) but also arise from a number of indoor sources (e.g. cigarette smoke, building materials, personal products). Aerosol particles can deposit in ventilation ducts and on surfaces of rooms or can be transported between zones; this can have serious effects in hospitals and buildings used by the pharmaceutical industry [2]. Deposition of airborne particles in museums and galleries can lead to perceptible soiling within a short time and ultimately result in damage to works of art.

The concentration of indoor aerosol particles can be reduced by mechanical ventilation using extract fans or by natural ventilation which allows air exchange between the indoor and the outdoor environment via windows and doorways. The distribution of fresh air and the total supply rate of fresh air are important aspects of natural ventilation [3]. The airflow estimated using tracer-gas techniques [4-5], is not sufficient to describe the removal of particles as particle deposition rate, particle type, size, source and concentration must be taken into consideration. This paper describes a detailed study of the flow of aerosol particles through large openings and the deposition characteristics of particles on different types of materials e.g. wood, aluminium foil and carpet.

2. THEORY

Generally room air is not perfectly mixed, therefore in any volume of room air, there are unequal portions of fresh air and air which has been resident in the room for a period of time (ie stale air). The freshness of air in a given volume may be described by the 'mean age' of air within it. The room-mean age-of-air is defined as the average value of the local mean ages of air for all points in a room [3]. This may be measured using the concentration decay technique. The method involves the initial injection of a tracer gas (e.g. SF₆) and particles (e.g. oil-smoke) into a zone and is followed by a period of mixing to establish a uniform concentration in the zone. The decay of SF₆ tracer-gas and smoke particles is then measured using suitable detectors over a given time interval. The rate of decrease of tracer-gas and smoke-particle concentration is given by the following equations:

$$C_{g(t)} = C_{g(t_0)} e^{-It} \quad (1)$$

$$C_{p(t)} = C_{p(t_0)} e^{-Pt} \quad (2)$$

If the concentrations of the tracer-gas and particles are plotted against elapsed time on semi-log paper, the negative slopes of the line are equal to I and P, respectively.

The room-average age-of-air $\langle \tau \rangle$ at location j can be determined [6] using the following equation :

$$\langle \tau \rangle = \frac{\text{First moment of measured area} + \text{First moment of residual area}}{\text{Measured area} + \text{Residual area}} \quad (3)$$

where:

$$\text{First moment of measured area} = 1/8 C_O \Delta\tau + 1/2 C_M \Delta\tau \tau_M + \sum_{j=1}^{M-1} C_j \tau_j \Delta\tau$$

$$\text{First moment of residual area} = C_M / \lambda_{exp} (\tau_M + 1/\lambda_{exp})$$

$$\text{Measured area} = 1/2(C_O + C_M) \Delta\tau + \sum_{j=1}^{M-1} C_j \Delta\tau$$

$$\text{Residual area} = C_M / \lambda_{exp}$$

3. EXPERIMENTAL

Experimental work was carried out using a room 11.6m x 3.65 m with a maximum height of 4.2m (Figure 1). The room was fitted with windows which allowed single-sided flows to be examined. SF₆ tracer-gas and oil-smoke particles were injected into the room and this was followed by a

mixing period during which desk fans were used. Multipoint -sampling units were then used to collect tracer-gas samples from the room for subsequent injection into infra-red gas analysers type BINOS 1000, manufactured by Rosemount Ltd, UK. The accuracy of the measurements was estimated to be within $\pm 5\%$.

Particle concentrations and sizes were measured using a laser-particle dust monitor type 1.102, manufactured by Grimm Ltd, Germany. The monitor is capable of measuring particle concentrations in the range 0.0001 - 500 mg/m^3 for particle size ranging between 0.5 - 10 μm in diameter with an accuracy of $\pm 5\%$.

Aerosol particles were injected into the room using a smoke generator. The generator has a microprocessor-controlled system capable of producing oil-smoke particles between 0.1 - 2 μm in diameter with a mass median diameter of $< 0.3 \mu\text{m}$.

4. RESULTS AND DISCUSSIONS

4.1 Measurements of tracer-gas and particle exchange rates

Experiments were performed in a room to determine tracer-gas and particle exchange rates for the following conditions:

- (i) One window fully-open
- (ii) Two windows fully-open

The experimental procedure involved injection of SF_6 tracer-gas and smoke particles in the room, Figure 1. After a mixing period of 15 minutes, simultaneous concentration measurements of tracer-gas and smoke particles (diameter 1 - 2 μm) were performed using the tracer-gas analyser and particle monitor, respectively. Samples were taken at six locations within the room at heights 0.8 and 1.2m from the floor to determine the local concentrations of tracer-gas and particles (see Figure 1). The average concentrations of tracer-gas and particles were also measured using multipoint sampling systems. A special sampling arrangement was used to reduce deposition of aerosol particles. The indoor and outdoor temperatures, windspeed and direction were monitored during the tests. Figures 2 - 4 show the variation of the concentration of particles and tracer-gas with time for condition (i). The particle and tracer-gas decay curves were found to be simple exponential functions for all conditions.

The local tracer (or particle)-exchange indicator ϵ_i was calculated using :

$$\varepsilon_i = \tau_n/\tau_p \times 100 \% \quad (4)$$

Results indicated that local age-of-tracer is higher than the average age-of-tracer. Local tracer-gas indicators were found to be in the ranges 0.72 - 0.92 and 0.7 - 1.16 for conditions (i) and (ii), respectively.

The local age-of-particles was found to be generally lower than the average age-of-particles. For condition (i), local particle-exchange indicators were found to be in the ranges 0.47 - 2.78 and 0.89 - 2.92 for $d > 1 \mu\text{m}$ and $d > 2 \mu\text{m}$, respectively.

The local average age-of-particles was found to be highest in the middle of the room. The local average age-of-particles was found to increase with increasing particle size. The age-of-tracer was greater than the age-of-particles.

Particle exchange rates were higher than tracer-gas exchange rates. The difference in tracer-gas and particle exchange rates is due to the deposition (or adsorption effect) of particles on the surfaces of the room. This was estimated using the following equation:

$$\alpha = \{P - I\} * V/A \quad (5)$$

For condition (i), the deposition rates were in the ranges 0.92 - 6.57 ($\mu\text{g}/\text{m}^2\text{h}$) and 0.83 - 3.85 ($\mu\text{g}/\text{m}^2\text{h}$) for $d > 1 \mu\text{m}$ and $d > 2 \mu\text{m}$, respectively.

4.2 Measurements in a lined chamber

Experiments were performed in a chamber at different ventilation rates. The chamber was lined with the following materials:

- (i) wood (unlined chamber)
- (ii) aluminium foil
- (iii) carpet

For each material SF_6 tracer-gas and oil-smoke particles were injected into the chamber. After a mixing period of 1 hour, simultaneous measurements of the concentrations of tracer-gas and oil-smoke particles were performed using the infra-red gas analyser and particle monitor, respectively. The tracer-gas and particle decay curves were found to be simple exponential functions for all conditions.

Table 3 shows experimental results for conditions (i) to (iii). Deposition rate, α , is obtained using Equation 4. Figures 5 - 7 show the variation of deposition rate with flow rate for wood, aluminium foil and carpet, respectively. The deposition rate on all materials was found to be dependent on the size of the particles. Particle exchange rates on wood and carpet was found to increase at air exchange rates above 0.9 h^{-1} and 0.8 h^{-1} , respectively. For aluminium, the deposition rate was found to be highest at an air exchange rate of 0.5 h^{-1} and then decreased. Similar results were obtained when R10 (silica oxide, SiO_2 , from Particle Technology Ltd., UK) aerosol particles were used instead of oil-smoke particles.

The deposition rate on wood and carpet was found to be several orders of magnitude higher than on aluminium foil. Low deposition rate on aluminium indicates that it would be possible to reduce particle deposition in buildings by using highly polished metal surfaces. The results also indicate that ventilation rate in buildings has a strong effect on particle deposition.

Table 3 also shows the average deposition velocity of the oil-smoke particles for various tests. The results indicated that the deposition velocity increased with increasing particle size. Deposition velocities in the chamber lined with wood and carpet were significantly higher than when aluminium foil was used.

5. CONCLUSIONS

- (i) The results showed that particle exchange rates were higher than tracer-gas exchange rates. This was due to the deposition effect of particles on the surfaces of the room and chamber.
- (ii) Deposition rate was found to be dependent on the size of particles and on the type of lining material used.
- (iii) The results also indicated that ventilation rate in buildings has a strong effect on deposition of particles.
- (iv) The room age-of-tracer was found to be greater than room age-of-particles.

REFERENCES

1. TURIEL, I.
"Indoor air quality and human health"
Stanford University Press, Stanford, California, 1985

2. FARANCE, K. and WILKINSON, J.
"Dusting down suspended particles"
Building Services, Vol 12, 1990, p 45-46
3. WALKER, R. R. and WHITE, M. K.
"Single-sided natural ventilation - How deep an office?"
Building Services Engineering Research and Technology, Vol 13(4),
1992, p 231-236
4. RIFFAT, S. B.
"Comparison of tracer-gas techniques for measuring airflow in a
duct"
J. Institute of Energy, Vol LXIII, 545, 1990, p 18 -21
5. ADAM, N. M. and RIFFAT, S. B.
"Deposition of aerosol particles in buildings"
CLIMA 2000 Conference, London, UK, November 1-3, 1993
(accepted for publication)
6. Grieve, P.W.
"Measuring ventilation using tracer-gases"
Bruel and Kjaer, Technical Note , October, 1989, p 28

Table 1 Experimental Results; One Window Fully-open

| H | X | τ_{LT} | τ_{AT} | ϵ_i | $\omega_s (\omega_D)$ | ΔT |
|-----|----|-------------|-------------|--------------|-----------------------|------------|
| 1.2 | 1 | 15.46 | 14.29 | 0.92 | 3.44 (92) | 17 |
| | 5 | 19.02 | 14.29 | 0.75 | 3.44 (92) | 17 |
| 1.2 | 6 | 15.46 | 11.43 | 0.74 | 4.12(138) | 14 |
| | 11 | 14.45 | 11.43 | 0.79 | 4.12(138) | 14 |
| 1.2 | 4 | 13.62 | 10.02 | 0.74 | 4.2 (124) | 15 |
| | 9 | 12.76 | 10.02 | 0.79 | 4.2 (124) | 15 |
| 0.8 | 4 | 14.61 | 10.56 | 0.72 | 4.2 (92) | 14 |
| | 9 | 13.01 | 10.56 | 0.81 | 4.2 (92) | 14 |
| 0.8 | 6 | 12.83 | 11.18 | 0.87 | 3.3 (105) | 19 |
| | 11 | 13.44 | 11.18 | 0.83 | 3.3 (105) | 19 |

| $d > 1 \mu m$ | | | | $d > 2 \mu m$ | | | |
|---------------|-------------|--------------|----------|---------------|-------------|--------------|----------|
| τ_{LP} | τ_{AP} | ϵ_i | α | τ_{LP} | τ_{AP} | ϵ_i | α |
| 10.57 | 12.12 | 1.15 | 1.58 | 12.50 | 13.21 | 1.06 | 1.06 |
| 14.51 | 12.12 | 0.84 | 1.38 | 14.88 | 13.21 | 0.89 | 1.52 |
| 12.45 | 5.83 | 0.47 | 0.92 | 10.96 | 10.03 | 0.92 | 0.84 |
| 6.94 | 5.83 | 0.84 | 0.94 | 8.97 | 10.03 | 1.12 | 1.16 |
| 8.48 | 15.94 | 1.88 | 1.18 | 9.72 | 20.19 | 2.08 | 0.83 |
| 5.74 | 15.94 | 2.78 | 6.57 | 6.91 | 20.19 | 2.92 | 3.54 |
| 7.87 | 10.14 | 1.29 | 3.43 | 9.05 | 10.07 | 1.11 | 1.63 |
| 9.88 | 10.14 | 1.03 | 1.39 | 10.6 | 10.07 | 0.95 | 2.48 |
| 8.07 | 8.63 | 1.07 | 2.50 | 8.06 | 10.78 | 1.34 | 2.34 |
| 5.07 | 8.63 | 1.70 | 2.83 | 5.89 | 10.78 | 1.83 | 3.85 |

Table 2 Experimental Results; Two Windows Fully-open

| H | X | τ_{LT} | τ_{AT} | ϵ_i | $\omega_s (\omega_D)$ | ΔT |
|-----|----|-------------|-------------|--------------|-----------------------|------------|
| 1.2 | 1 | 7.33 | 6.60 | 0.90 | 3.84(67) | 13 |
| | 6 | 8.72 | 6.60 | 0.76 | 384(67) | 13 |
| 1.2 | 4 | 7.34 | 5.61 | 0.76 | 4.91(122) | 15 |
| | 9 | 6.96 | 5.61 | 0.81 | 4.91(122) | 15 |
| 1.2 | 5 | 8.45 | 6.39 | 0.76 | 4.34(123) | 12 |
| | 11 | 7.86 | 6.39 | 0.81 | 4.34(123) | 12 |
| 0.8 | 5 | 9.31 | 7.88 | 0.85 | 2.75(122) | 16 |
| | 9 | 6.82 | 7.88 | 1.16 | 2.75(122) | 16 |
| 0.8 | 5 | 7.68 | 5.38 | 0.70 | 2.75(323) | 16 |
| | 11 | 7.46 | 5.38 | 0.72 | 2.75(323) | 16 |

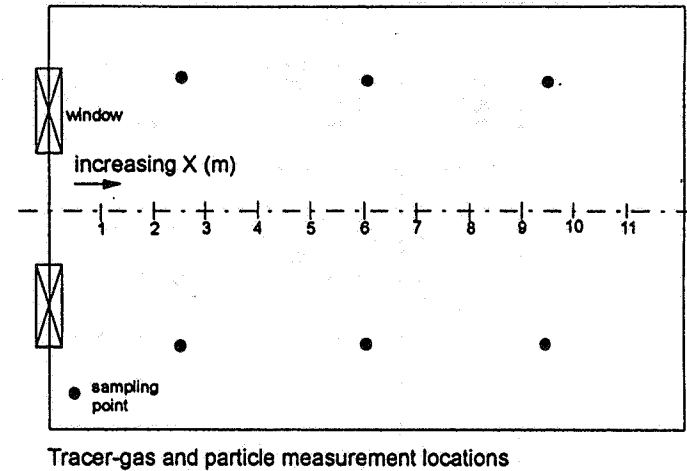
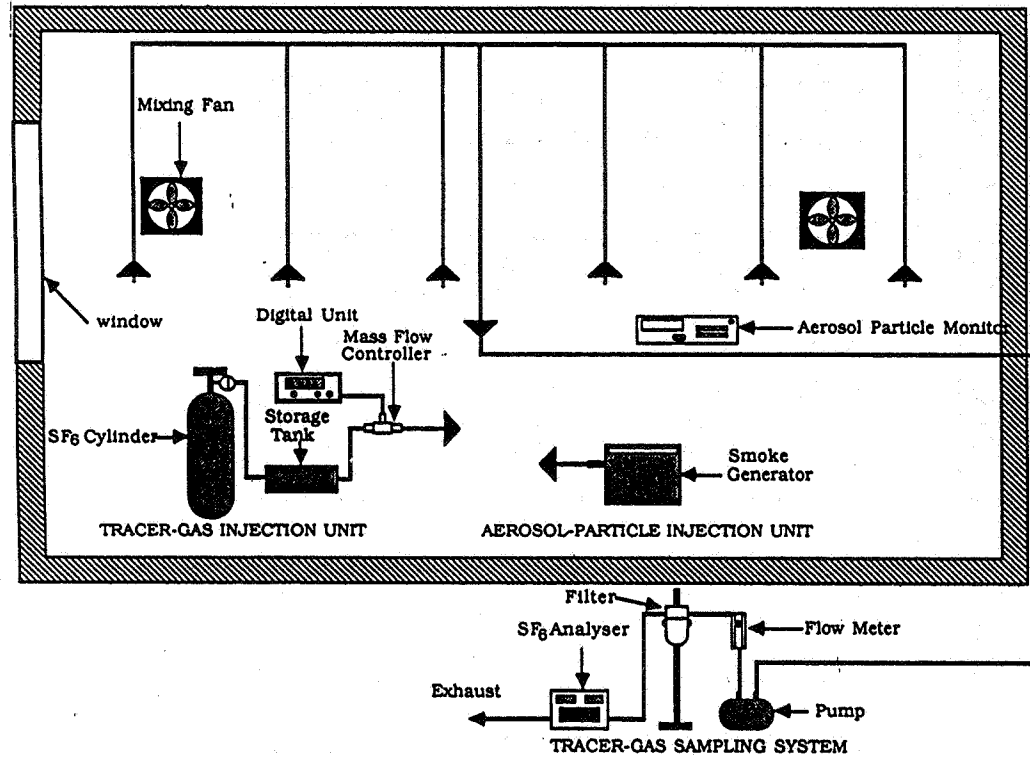
| d > 1 μm | | | | d > 2 μm | | | |
|---------------------|-------------|--------------|----------|---------------------|-------------|--------------|----------|
| τ_{LP} | τ_{AP} | ϵ_i | α | τ_{LP} | τ_{AP} | ϵ_i | α |
| 1.29 | 2.51 | 1.95 | 2.20 | 11.10 | 5.29 | 0.48 | 0 |
| 6.13 | 2.51 | 0.41 | 2.71 | 6.89 | 5.29 | 0.77 | 1.67 |
| 10.51 | 16.78 | 1.60 | 0 | 10.33 | 24.14 | 2.34 | 0 |
| 4.98 | 16.78 | 3.37 | 3.58 | 7.12 | 24.14 | 3.39 | 0.01 |
| 8.00 | 5.35 | 0.67 | 2.66 | 6.75 | 6.94 | 1.03 | 1.13 |
| 3.50 | 5.35 | 1.53 | 1.44 | 5.34 | 6.94 | 1.30 | 3.32 |
| *n.a. | 5.88 | n.a. | n.a. | n.a. | 7.47 | n.a. | n.a. |
| 7.36 | 5.88 | 0.80 | 0 | 4.26 | 7.47 | 1.75 | 2.66 |
| 3.90 | 4.63 | 1.19 | 5.40 | 4.75 | 5.68 | 1.20 | 5.23 |
| 3.70 | 4.63 | 1.25 | 4.52 | 3.41 | 5.68 | 1.67 | 4.08 |

*n.a. not available

Table 3 Results For Lined Chamber

| Material | I, (h ⁻¹) | P, (µg/m ³ h) | | |
|-----------|-----------------------|--------------------------|--------|--------|
| | | d > .5µm | d >1µm | d >2µm |
| wood | 0.308 | 0.313 | 0.413 | 1.309 |
| | 0.595 | 1.076 | 1.203 | 2.231 |
| | 0.994 | 1.099 | 1.765 | 2.280 |
| | 1.359 | 3.773 | 2.517 | 6.204 |
| aluminium | 0.199 | 0.369 | 0.480 | 0.541 |
| | 0.637 | 0.993 | 1.129 | 1.348 |
| | 1.020 | 1.138 | 1.208 | 1.411 |
| | 1.314 | 1.146 | 1.443 | 1.653 |
| carpet | 0.303 | 1.185 | 1.572 | 1.993 |
| | 0.583 | 1.244 | 1.546 | 1.766 |
| | 0.839 | 1.597 | 1.876 | 2.160 |
| | 1.004 | 3.650 | 3.853 | 4.564 |

| α, (µg/m ² h) | | | V _D (x10 ⁻⁶ cm/s) | | |
|--------------------------|-------|-------|---|-------|-------|
| d>.5µm | d>1µm | d>2µm | d>.5µm | d>1µm | d>2µm |
| 0.001 | 0.021 | 0.200 | 0.002 | 0.149 | 3.740 |
| 0.096 | 0.122 | 0.327 | 0.464 | 4.893 | 56.46 |
| 0.021 | 0.154 | 0.257 | 0.091 | 2.077 | 10.49 |
| 0.483 | 0.232 | 0.969 | 4.576 | 11.56 | 384.6 |
| 0.034 | 0.056 | 0.068 | 0.071 | 0.146 | 0.219 |
| 0.071 | 0.098 | 0.142 | 0.119 | 0.190 | 0.342 |
| 0.024 | 0.038 | 0.078 | 0.080 | 0.106 | 0.257 |
| 0 | 0.026 | 0.068 | 0 | 0.036 | 0.110 |
| 0.177 | 0.254 | 0.338 | 1.289 | 2.160 | 4.891 |
| 0.132 | 0.193 | 0.237 | 1.683 | 3.733 | 7.555 |
| 0.152 | 0.207 | 0.264 | 1.026 | 1.774 | 3.420 |
| 0.529 | 0.570 | 0.712 | 238.4 | 545.9 | 989.0 |



Tracer-gas and particle measurement locations

Figure 1 Schematic diagram of room and instrumentation

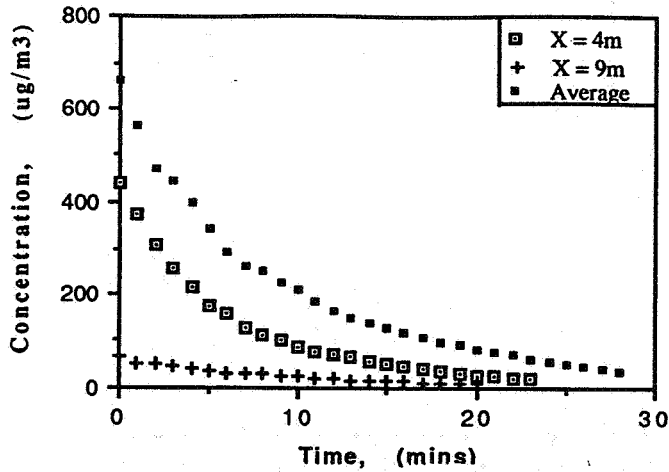


Figure 2 Variation of particle concentration with time, one window fully-open, $H=0.8m$, $d>1\mu m$

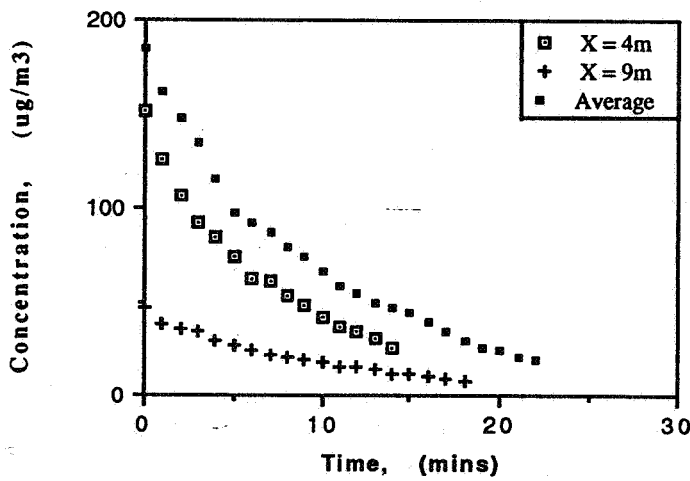


Figure 3 Variation of particle concentration with time, one window fully-open, $H=0.8m$, $d>2\mu m$

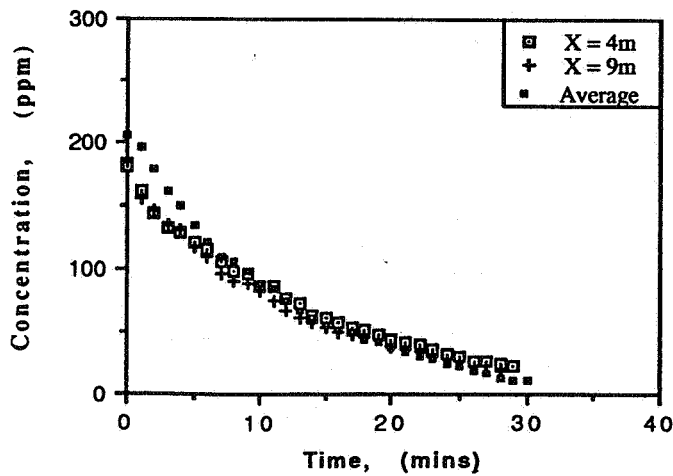


Figure 4 Variation of tracer-gas concentration with time, one window fully-open, $H=0.8m$

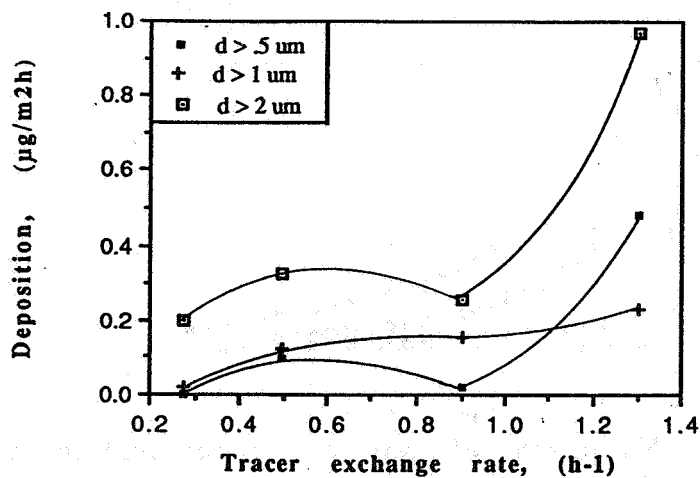


Figure 5 Variation of particle deposition rate with tracer-gas exchange rate, wood

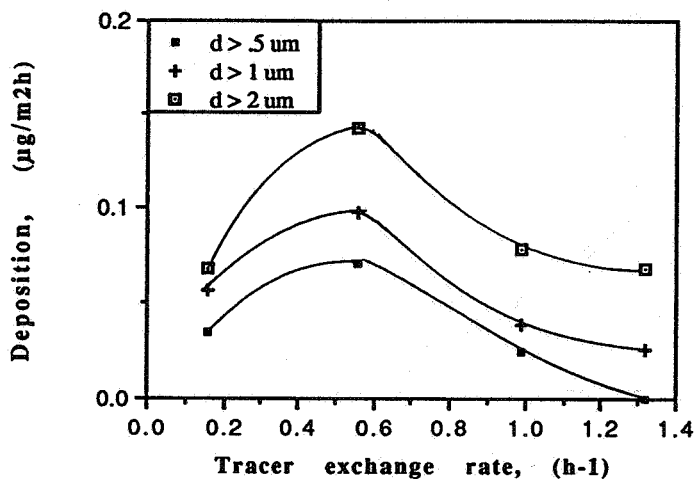


Figure 6 Variation of particle deposition rate with tracer-gas exchange rate, aluminium

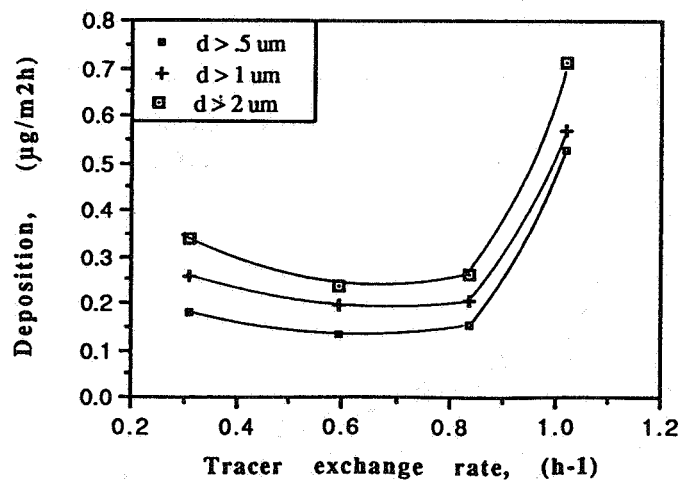


Figure 7 Variation of particle deposition rate with tracer-gas exchange rate, carpet